

# Classical aspects of quantum fields far from equilibrium

Gert Aarts and Jürgen Berges

*Institut für Theoretische Physik, Philosophenweg 16, 69120 Heidelberg, Germany*  
(July 11, 2001)

We consider the time evolution of nonequilibrium quantum scalar fields in the  $O(N)$  model, using the next-to-leading order  $1/N$  expansion of the  $2PI$  effective action. A comparison with exact numerical simulations in  $1+1$  dimensions in the classical limit shows that the  $1/N$  expansion gives quantitatively precise results already for moderate values of  $N$ . For sufficiently high initial occupation numbers the time evolution of quantum fields is shown to be accurately described by classical physics. Eventually the correspondence breaks down due to the difference between classical and quantum thermal equilibrium.

PACS numbers: 11.15.Pg, 11.10.Wx, 05.70.Ln

HP-THEP-01-28

In recent years we have witnessed an enormous increase of interest in the dynamics of quantum fields out of equilibrium. Much progress has been achieved for systems close to thermal equilibrium or with effective descriptions based on a separation of scales in the weak coupling limit [1]. Current and upcoming relativistic heavy-ion collision experiments provide an important motivation to find controlled nonperturbative approximation schemes which yield a quantitative description of far-from-equilibrium phenomena from first principles.

Practicable nonperturbative approximations may be based on the two-particle irreducible ( $2PI$ ) generating functional for Green's functions [2]. Recently, a systematic  $1/N$  expansion of the  $2PI$  effective action has been proposed for a scalar  $O(N)$  symmetric quantum field theory [3]. This nonperturbative approach extends previous successful descriptions of the large-time behavior of quantum fields [4,5], which employ the loop expansion of the  $2PI$  effective action relevant at weak couplings [2,6]. At next-to-leading order (NLO) the  $1/N$  expansion of the  $2PI$  effective action has been solved for the quantum theory in  $1+1$  dimensions [3]. The approach overcomes the problem of a secular time evolution, which is encountered in the standard  $1/N$  expansion of the  $1PI$  effective action beyond leading order [7].

Our purpose in this Letter is to establish that the  $1/N$  expansion at NLO gives quantitatively precise results already for moderate values of  $N$ . We therefore have a small nonperturbative expansion parameter at hand and a controlled description of far-from-equilibrium dynamics becomes possible. As an application we compare quantum and classical evolution and demonstrate that the nonequilibrium quantum field theory can be described by its classical field theory limit for sufficiently high initial occupation numbers. We show that eventually the correspondence breaks down due to the difference between classical and quantum thermal equilibrium.

Employing the classical statistical field theory limit, we compare the  $1/N$  expansion of the  $2PI$  effective action at NLO with the *exact* result, which includes all orders in  $1/N$ . The time evolution of classical nonequilibrium Green's functions can be calculated exactly, up to controlled numerical uncertainties, by integrating the

microscopic field equations of motion. This allows one to obtain a direct comparison [8]. Apart from benchmarking approximation schemes employed in quantum field theory, the importance of the classical field limit for the approximate description of nonequilibrium quantum fields is manifest.

*$2PI$  effective action.* We consider a real  $N$ -component scalar quantum field theory with a  $\lambda(\phi_a\phi_a)^2/(4!N)$  interaction in the symmetric phase ( $a = 1, \dots, N$ ). The  $2PI$  generating functional for Green's functions can be parametrized as [2]

$$\Gamma[G] = \frac{i}{2} \text{Tr} \ln G^{-1} + \frac{i}{2} \text{Tr} G_0^{-1} G + \Gamma_2[G] + \text{const}, \quad (1)$$

where  $G_0^{-1} = i(\square + m^2)$  denotes the free inverse propagator. The  $2PI$  contribution  $\Gamma_2[G]$  can be computed from a systematic  $1/N$  expansion of the  $2PI$  effective action [3]. Writing  $\Gamma_2[G] = \Gamma_2^{\text{LO}}[G] + \Gamma_2^{\text{NLO}}[G] + \dots$  the LO and NLO contributions are given by [3,9]

$$\Gamma_2^{\text{LO}}[G] = -\frac{\lambda}{4!N} \int_{\mathcal{C}} d^{d+1}x G_{aa}(x, x) G_{bb}(x, x), \quad (2)$$

$$\Gamma_2^{\text{NLO}}[G] = \frac{i}{2} \text{Tr}_{\mathcal{C}} \ln[\mathbf{B}(G)]. \quad (3)$$

Here  $\mathcal{C}$  denotes the Schwinger-Keldysh contour along the real time axis [10] and

$$\mathbf{B}(x, y; G) = \delta_{\mathcal{C}}^{d+1}(x - y) + i \frac{\lambda}{6N} G_{ab}(x, y) G_{ab}(x, y). \quad (4)$$

The nonlocal four-point vertex at NLO is given by  $\frac{\lambda}{6N} \mathbf{B}^{-1}$  [3]. In absence of external sources the evolution equation for  $G$  is determined by [2]

$$\frac{\delta \Gamma[G]}{\delta G_{ab}(x, y)} = 0. \quad (5)$$

We consider the  $O(N)$  symmetric case, such that  $G_{ab}(x, y) = G(x, y) \delta_{ab}$ . In the following we solve Eq. (5), using Eqs. (1)–(4) without further approximations numerically in  $1+1$  dimensions [3]. We compare the outcome with results in the classical field theory limit, using

both the NLO classical approximation and the “exact” Monte Carlo calculation [8] as described below.

*Nonequilibrium time evolution.* To formulate the nonequilibrium dynamics as an initial-value problem, we decompose the full two-point function using the identity  $G(x, y) = F(x, y) - (i/2)\rho(x, y) \text{sign}_c(x^0 - y^0)$  where  $F$  is the symmetric or statistical two-point function and  $\rho$  denotes the spectral function [5]. Following Refs. [5, 3], Eq. (5) can be written as

$$\begin{aligned} [\square_x + M^2(x)] F(x, y) &= - \int_0^{x^0} dz^0 \int d\mathbf{z} \Sigma_\rho(x, z) F(z, y) \\ &\quad + \int_0^{y^0} dz^0 \int d\mathbf{z} \Sigma_F(x, z) \rho(z, y), \quad (6) \\ [\square_x + M^2(x)] \rho(x, y) &= - \int_{y^0}^{x^0} dz^0 \int d\mathbf{z} \Sigma_\rho(x, z) \rho(z, y). \end{aligned}$$

At NLO in the  $1/N$  expansion the effective mass term  $M^2(x)$  is given by  $M^2(x) = m^2 + \lambda \frac{N+2}{6N} F(x, x)$  and the self energies are [3]

$$\Sigma_F(x, y) = -\frac{\lambda}{3N} \left[ F(x, y) I_F(x, y) - \frac{1}{4} \rho(x, y) I_\rho(x, y) \right], \quad (7)$$

$$\Sigma_\rho(x, y) = -\frac{\lambda}{3N} \left[ \rho(x, y) I_F(x, y) + F(x, y) I_\rho(x, y) \right]. \quad (8)$$

Here the functions  $I_F$  and  $I_\rho$  resum an infinite chain of bubble diagrams,

$$\begin{aligned} I_F(x, y) &= -\frac{\lambda}{3} \Pi_F(x, y) + \frac{\lambda}{3} \int_0^{x^0} dz^0 \int d\mathbf{z} I_\rho(x, z) \Pi_F(z, y) \\ &\quad - \frac{\lambda}{3} \int_0^{y^0} dz^0 \int d\mathbf{z} I_F(x, z) \Pi_\rho(z, y), \\ I_\rho(x, y) &= -\frac{\lambda}{3} \Pi_\rho(x, y) + \frac{\lambda}{3} \int_{y^0}^{x^0} dz^0 \int d\mathbf{z} I_\rho(x, z) \Pi_\rho(z, y), \end{aligned}$$

with

$$\Pi_F(x, y) = -\frac{1}{2} \left( F^2(x, y) - \frac{1}{4} \rho^2(x, y) \right), \quad (9)$$

$$\Pi_\rho(x, y) = -F(x, y) \rho(x, y). \quad (10)$$

*Classical field theory limit.* The classical statistical field theory limit of a scalar quantum field theory has been studied extensively in the literature. An analysis along the lines of Refs. [11–14] shows that all equations (6)–(10) remain the same in the classical limit except for differing expressions for the statistical components of the self energy

$$\Sigma_F(x, y) \xrightarrow{\text{classical limit}} -\frac{\lambda}{3N} F(x, y) I_F(x, y), \quad (11)$$

$$\Pi_F(x, y) \xrightarrow{\text{classical limit}} -\frac{1}{2} F^2(x, y). \quad (12)$$

The latter expressions are given by Eqs. (7) and (9) in the quantum theory. One observes that the classical self

energies are obtained from the expressions in the quantum theory by dropping terms with two spectral ( $\rho$ -type) components compared to two statistical ( $F$ -type) functions. This particular relationship has been studied in great detail in thermal equilibrium and corresponds to retaining only contributions that are of leading order in  $\hbar$ . It has been systematized in terms of Feynman rules for classical and quantum theories using the Keldysh formulation with appropriate interaction vertices [11]. Note that the classical spectral function is obtained from the quantum one by replacing  $-i$  times the commutator by the classical Poisson bracket. A comparison of the classical limit in the current approximation for  $N = 1$  has been studied in Ref. [14].

*Monte Carlo approach.* An “exact” nonperturbative solution of the evolution of classical correlation functions in the  $O(N)$  model can be obtained numerically in a straightforward manner [8]. Initial conditions are determined from a probability functional on classical phase-space. The subsequent time evolution is solved numerically using the classical equations of motion. In the figures presented below, we have sampled 50000-80000 independent initial conditions to approximate the exact evolution.

*Far from equilibrium evolution.* We consider a system that is invariant under space translations and work in momentum space. We choose a Gaussian initial state such that a specification of the initial two-point functions is sufficient. The quantum (classical) spectral function at initial time is completely determined from the equal-time commutation relations (Poisson brackets). For the symmetric two-point function we take  $F(0, 0; p) = [n_0(p) + \frac{1}{2}]/\omega_p$ , with the initial particle number  $n_0(p) = n_{\text{ts}}(p) + n_B(p)$  representing a peaked “tsunami”  $n_{\text{ts}}(p) = \mathcal{A} \exp[-\frac{1}{2\sigma^2}(|p| - |p_{\text{ts}}|)^2]$  in a thermal background  $n_B(p) = [\exp(\omega_p/T_0) - 1]^{-1}$  [15, 5, 3]. Such an initial state is reminiscent of two colliding wave packets [15] and provides a far-from-equilibrium initial condition. We emphasize that these initial conditions can be implemented both in a quantum and a classical theory. The initial mode energy is given by  $\omega_p = (p^2 + M^2)^{1/2}$  where  $M$  is the one-loop renormalized mass in presence of the nonequilibrium medium, determined from the one-loop gap equation. As a renormalization condition we choose the one-loop renormalized mass in vacuum  $m_R \equiv M|_{n_0=0} = 1$  as our dimensionful scale. The results shown below are obtained using a fixed coupling constant  $\lambda/m_R^2 = 30$ .

*Convergence of NLO and Monte Carlo results.* In Fig. 1 we present the two-point function  $F(t, 0; p = 0)$  in the classical field theory limit for three values of  $N$ . All other parameters are kept constant. The figure compares the time evolution using the  $1/N$  expansion of the  $2PI$  effective action to NLO and the Monte Carlo calculation that includes all orders in  $1/N$ . One observes that the approximate time evolution of the correlation function shows a rather good agreement with the exact

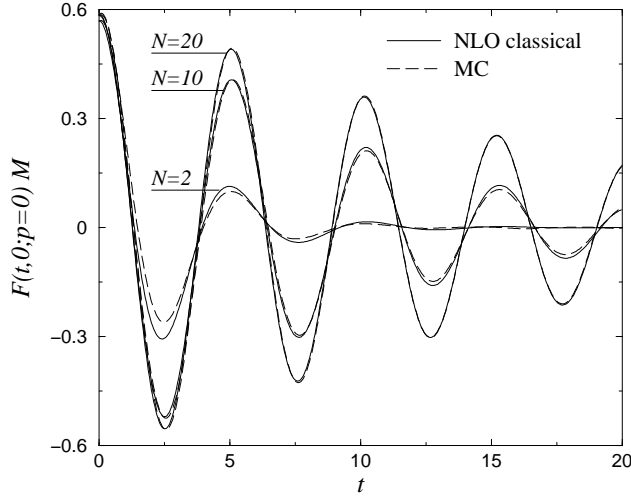


FIG. 1. Unequal time two-point function  $F(t, 0; p = 0)$  at zero momentum times the initial mass  $M$  for  $N = 2, 10, 20$ . The full lines show results from the NLO classical evolution and the dashed lines from the exact classical evolution (MC). For  $N = 20$  the NLO and exact evolution can hardly be distinguished.

result even for small values of  $N$  (note that the effective four-point coupling is strong,  $\lambda/6N = 2.5m_R^2$  for  $N = 2$ ). For  $N = 20$  the exact and NLO evolution can hardly be distinguished. A very sensitive quantity to compare is the damping rate  $\gamma$ , which is obtained from an exponential fit to the envelope of  $F(t, 0; p = 0)$ . The systematic convergence of the NLO and the Monte Carlo result as a function of  $1/N$  can be observed in Fig. 2. The quantitatively accurate description of far from equilibrium processes within the NLO approximation of the  $2PI$  effective action is manifest.

*Classical behavior of nonequilibrium quantum fields.* In Fig. 2 we also show the damping rate from the quantum evolution, using the same initial conditions and parameters. We observe that the damping in the quantum theory differs and, in particular, is reduced compared to the classical result. In the limit  $N \rightarrow \infty$  damping of the unequal-time correlation function  $F(t, 0; p)$  goes to zero since the nonlocal part of the self energies (7)–(8) vanishes and scattering is absent. In this limit there is no difference between evolution in a quantum and classical statistical field theory.

For finite  $N$  scattering is present and quantum and classical evolution differ in general. However, the classical field approximation may be expected to become a reliable description for the quantum theory if the number of field quanta in each field mode is sufficiently high. We observe that increasing the initial particle number density leads to a convergence of quantum and classical time evolution at not too late times. In Fig. 3 we present the time evolution of the equal-time correlation function  $F(t, t; p)$  for several momenta  $p$  and  $N = 10$ . Here the

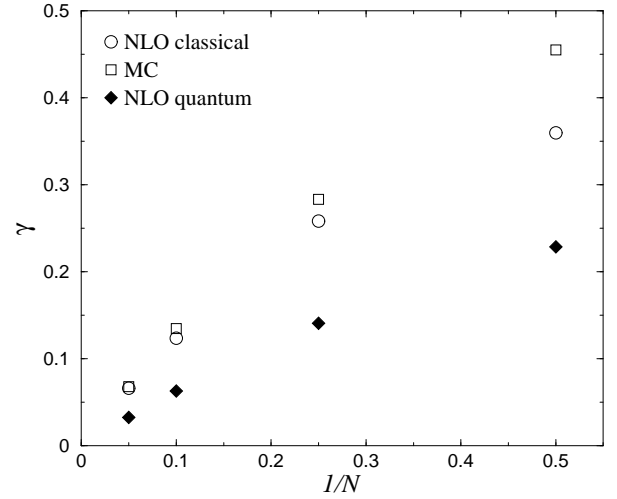


FIG. 2. Nonequilibrium damping rates extracted from  $F(t, 0; p = 0)$  shown in Fig. 1 as a function of  $1/N$ . Open symbols represent exact and NLO classical evolution. One observes a rapid convergence of the  $1/N$  expansion at NLO to the exact MC result. The quantum results are shown with full symbols. In the quantum theory the damping rate is reduced compared to the classical theory.

particle density  $\int \frac{dp}{2\pi} n_0(p)/M = 1.2$  is six times as high as in Figs. 1, 2 and, in contrast to the latter, quantum and classical evolution at NLO follow each other rather closely. For an estimate of the NLO truncation error we also give the MC result for  $N = 10$  showing a quantitative agreement with the classical NLO evolution both at early and later times.

*Quantum versus classical equilibration.* From Fig. 3 one observes that the initially highly occupied “tsunami” modes ( $p_{ts}/m_R = 2.5$ ) “decay” as time proceeds and the low momentum modes become more and more populated. At late times the classical theory [16, 8] and the quantum theory [4, 3] approach their respective thermal equilibrium distribution. Since classical and quantum thermal equilibrium are distinct the classical and quantum time evolutions have to deviate at sufficiently late times, irrespective of the initial particle number density per mode. Differences in the particle number distribution can be conveniently discussed using the inverse slope parameter  $T(t, p) \equiv -n(t, \epsilon_p)[n(t, \epsilon_p) + 1](dn/d\epsilon)^{-1}$  for a given time-evolving particle number distribution  $n(t, \epsilon_p)$  and dispersion relation  $\epsilon_p(t)$  [3]. Following Ref. [5] we define the effective particle number as  $n(t, \epsilon_p) + \frac{1}{2} \equiv [F(t, t'; p) \partial_t \partial_{t'} F(t, t'; p)]^{1/2}|_{t=t'}$  and mode energy by  $\epsilon_p(t) \equiv [\partial_t \partial_{t'} F(t, t'; p)/F(t, t'; p)]^{1/2}|_{t=t'}$ , which coincide with the usual free-field definition for  $\lambda \rightarrow 0$ . For a Bose-Einstein distributed particle number the parameter  $T(t, p)$  corresponds to the (momentum independent) temperature  $T(t, p) = T_{eq}$ . In the classical limit the inverse slope  $T(t, p)$  as defined above remains momentum dependent.

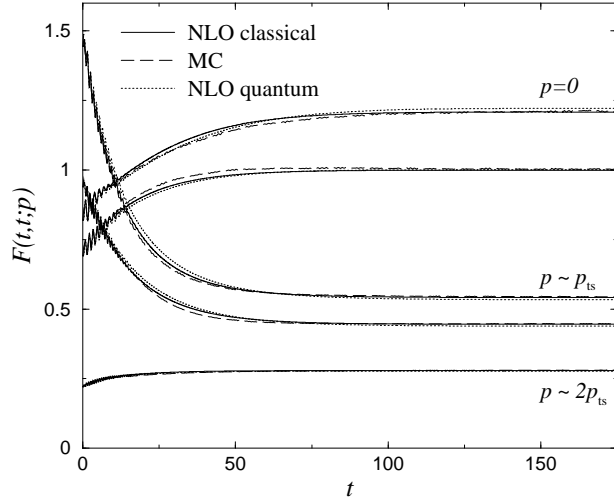


FIG. 3. Nonequilibrium evolution of the equal-time two-point function  $F(t, t; p)$  for  $N = 10$  for various momenta  $p$ . One observes a good agreement between the exact MC (dashed) and the NLO classical result (full). The quantum evolution is shown with dotted lines. The initial particle density is six times as high as in Figs. 1,2. At these high densities, the difference between quantum and classical evolution is small.

In Fig. 4 we plot the function  $T(t, p)$  for  $p_{\text{low}} \simeq 0$  and  $p_{\text{high}} \simeq 2p_{\text{ts}}$ . Initially one observes a very different behavior of  $T(t, p)$  for the low and high momentum modes, indicating that the system is far from equilibrium. Note that classical and quantum evolution agree very well for sufficiently high initial particle number density. However, at later times the difference between quantum and classical evolution becomes visible. The quantum evolution approaches quantum thermal equilibrium with a momentum independent inverse slope  $T = 4.7m_R$ . In contrast, in the classical limit the slope parameter remains momentum dependent and the system relaxes towards classical thermal equilibrium [17].

We thank W. Wetzel for continuous support in computational resources. This work was supported by the TMR network *Finite Temperature Phase Transitions in Particle Physics*, EU contract no. FMRX-CT97-0122.

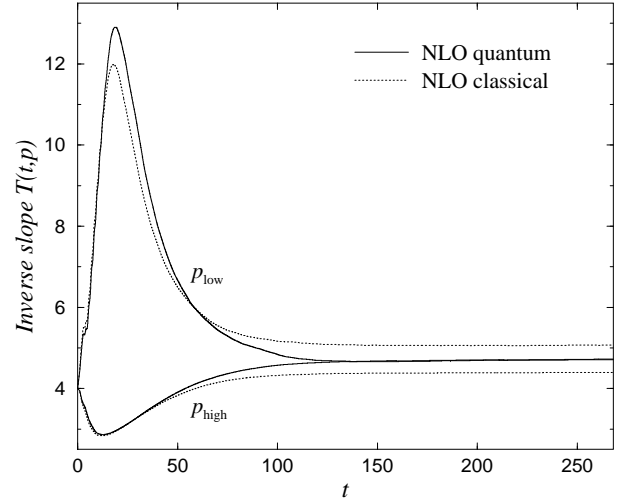


FIG. 4. Time dependence of the inverse slope  $T(t, p)$ , as defined in the text. When quantum thermal equilibrium is approached, all modes get equal inverse slope. In contrast, for classical thermal equilibrium the inverse slope is momentum dependent with  $T(p_{\text{low}}) > T(p_{\text{high}})$ .

[1] For recent reviews, see e.g. D. Bödeker, Nucl. Phys. Proc. Suppl. **94** (2001) 61 [hep-lat/0011077]; J. Blaizot, E. Iancu, hep-ph/0101103.  
[2] J. M. Cornwall, R. Jackiw, E. Tomboulis, Phys. Rev. **D10** (1974) 2428; see also J.M. Luttinger, J.C. Ward, Phys. Rev. **118** (1960) 1417; G. Baym, Phys. Rev. **127** (1962) 1391.  
[3] J. Berges, Nucl. Phys. **A699** (2002) 833 [hep-ph/0105311].  
[4] J. Berges, J. Cox, Phys. Lett. **B517** (2001) 369 [hep-ph/0006160].

[5] G. Aarts, J. Berges, Phys. Rev. **D64** (2001) 105010 [hep-ph/0103049].  
[6] E. Calzetta, B. L. Hu, Phys. Rev. **D37** (1988) 2878; K. Chou, Z. Su, B. Hao, L. Yu, Phys. Rept. **118** (1985) 1.  
[7] L. M. Bettencourt, C. Wetterich, Phys. Lett. **B430** (1998) 140 [hep-ph/9712429], hep-ph/9805360; B. Mihaila, T. Athan, F. Cooper, J. Dawson, S. Habib, Phys. Rev. **D62**, 125015 (2000) [hep-ph/0003105].  
[8] G. Aarts, G. F. Bonini, C. Wetterich, Phys. Rev. **D63** (2001) 025012 [hep-ph/0007357].  
[9] See also the “BVA” ansatz for quantum oscillators in B. Mihaila, F. Cooper, J. F. Dawson, Phys. Rev. D **63**, 096003 (2001) [hep-ph/0006254]. For vanishing field expectation value  $\langle \phi \rangle$  the BVA approximation corresponds to the  $1/N$  expansion of the  $2PI$  effective action at NLO.  
[10] J. Schwinger, J. Math. Phys. **2** (1961) 407; L. V. Keldysh, Zh. Eksp. Teor. Fiz. **47** (1964) 1515.  
[11] G. Aarts, J. Smit, Phys. Lett. **B393** (1997) 395 [hep-ph/9610415]; *ibid.* Nucl. Phys. **B511** (1998) 451 [hep-ph/9707342]; G. Aarts, B. Nauta, C. G. van Weert, Phys. Rev. **D61** (2000) 105002 [hep-ph/9911463].  
[12] W. Buchmüller, A. Jakovác, Phys. Lett. **B407** (1997) 39.  
[13] F. Cooper, A. Khare, H. Rose, Phys. Lett. **B515** (2001) 463 [hep-ph/0106113].  
[14] K. Blagoev, F. Cooper, J. Dawson, B. Mihaila, Phys. Rev. **D64** (2001) 125003 [hep-ph/0106195].  
[15] R. D. Pisarski, hep-ph/9710370; D. Boyanovsky, H. J. de Vega, R. Holman, S. Prem Kumar, R. D. Pisarski, Phys. Rev. **D57** (1998) 3653 [hep-ph/9711258].  
[16] G. Aarts, G. F. Bonini, C. Wetterich, Nucl. Phys. **B587** (2000) 403 [hep-ph/0003262].  
[17] We have verified that in the classical field theory limit the “classical mode temperature”  $\partial_t \partial_{t'} F(t, t'; p)|_{t=t'}$  [16] becomes independent of  $p$  at very late times, as expected from classical equipartition.